

AD-A197 460

DTIC FILE COPY

4

The Effects of Chemistry and Crystal Structure on the Lubrication Properties of Sputtered MoS₂ Films

PAUL D. FLEISCHAUER and R. BAUER
Chemistry and Physics Laboratory
Laboratory Operations
The Aerospace Corporation
El Segundo, CA 90245

25 May 1988

Prepared for
SPACE DIVISION
AIR FORCE SYSTEMS COMMAND
Los Angeles Air Force Base
P.O. Box 92960, Worldway Postal Center
Los Angeles, CA 90009-2960


DTIC
ELECTE
JUL 26 1988
S E D


APPROVED FOR PUBLIC RELEASE;
DISTRIBUTION UNLIMITED

This report was submitted by The Aerospace Corporation, El Segundo, CA 90245, under Contract No. F04701-85-C-0086 with the Space Division, P.O. Box 92960, Worldway Postal Center, Los Angeles, CA 90009-2960. It was reviewed and approved for The Aerospace Corporation by S. Feuerstein, Director, Chemistry and Physics Laboratory. Lt Buford W. Shipley, SD/CWDE, was the project officer for the Mission-Oriented Investigation and Experimentation (MOIE) program.

This report has been reviewed by the Public Affairs Office (PAS) and is releasable to the National Technical Information Service (NTIS). At NTIS, it will be available to the general public, including foreign nationals.

This technical report has been reviewed and is approved for publication. Publication of this report does not constitute Air Force approval of the report's findings or conclusions. It is published only for the exchange and stimulation of ideas.


BUFORD W. SHIPLEY, Lt, USAF
MOIE Project Officer
SD/CWDE


RAYMOND M. LEONG, Major, USAF
Deputy Director, AFSTC West Coast Office
AFSTC/WCO OL-AB

UNCLASSIFIED

ADA197460

SECURITY CLASSIFICATION OF THIS PAGE

REPORT DOCUMENTATION PAGE

1a. REPORT SECURITY CLASSIFICATION Unclassified			1b. RESTRICTIVE MARKINGS	
2a. SECURITY CLASSIFICATION AUTHORITY			3. DISTRIBUTION/AVAILABILITY OF REPORT Approved for public release; distribution unlimited.	
2b. DECLASSIFICATION/DOWNGRADING SCHEDULE				
4. PERFORMING ORGANIZATION REPORT NUMBER(S) TR-0086A(2945-03)-3			5. MONITORING ORGANIZATION REPORT NUMBER(S) SD-TR-88-36	
6a. NAME OF PERFORMING ORGANIZATION The Aerospace Corporation Laboratory Operations		6b. OFFICE SYMBOL (if applicable)	7a. NAME OF MONITORING ORGANIZATION Space Division	
6c. ADDRESS (City, State, and ZIP Code) El Segundo, CA 90245			7b. ADDRESS (City, State, and ZIP Code) Los Angeles Air Force Base Los Angeles, CA 90009-2960	
8a. NAME OF FUNDING/SPONSORING ORGANIZATION		8b. OFFICE SYMBOL (if applicable)	9. PROCUREMENT INSTRUMENT IDENTIFICATION NUMBER F04701-85-C-0086	
8c. ADDRESS (City, State, and ZIP Code)			10. SOURCE OF FUNDING NUMBERS	
			PROGRAM ELEMENT NO.	PROJECT NO.
			TASK NO.	WORK UNIT ACCESSION NO.
11. TITLE (Include Security Classification) The Effects of Chemistry and Crystal Structure on the Lubrication Properties of Sputtered MoS ₂ Films				
12. PERSONAL AUTHOR(S) Fleischauer, Paul D., and Bauer, Reinhold				
13a. TYPE OF REPORT		13b. TIME COVERED FROM _____ TO _____	14. DATE OF REPORT (Year, Month, Day) 1988 May 25	15. PAGE COUNT 29
16. SUPPLEMENTARY NOTATION				
17. COSATI CODES			18. SUBJECT TERMS (Continue on reverse if necessary and identify by block number)	
FIELD	GROUP	SUB-GROUP	Solid lubricant, MoS ₂ lubricant, Crystal structure, MoS ₂	
19. ABSTRACT (Continue on reverse if necessary and identify by block number)				
<p>Lubricating films of MoS₂ have been prepared by sputter deposition onto steel substrates maintained at different temperatures. The surface chemical compositions and bulk structural properties of the films, before and after rubbing for various times in dry nitrogen gas, were determined by x-ray photoelectron spectroscopy and by x-ray diffraction, respectively. Film thicknesses, densities, and morphologies were also measured. Differences in these properties for the films prepared under different conditions provide insight into the mechanisms of film lubrication and failure. It is proposed that lubrication by MoS₂ films occurs through intercrystallite slip and that there is an optimal crystallite size that provides maximum wear life under particular application conditions. Methods are suggested for improving film performance, based on particle/crystallite size and lattice spacing arguments and on the electronic properties of MoS₂ and related compounds.</p>				
20. DISTRIBUTION/AVAILABILITY OF ABSTRACT <input checked="" type="checkbox"/> UNCLASSIFIED/UNLIMITED <input type="checkbox"/> SAME AS RPT. <input type="checkbox"/> DTIC USERS			21. ABSTRACT SECURITY CLASSIFICATION Unclassified	
22a. NAME OF RESPONSIBLE INDIVIDUAL			22b. TELEPHONE (Include Area Code)	22c. OFFICE SYMBOL

DD FORM 1473, 84 MAR

83 APR edition may be used until exhausted.
All other editions are obsolete.

SECURITY CLASSIFICATION OF THIS PAGE

UNCLASSIFIED

UNCLASSIFIED

SECURITY CLASSIFICATION OF THIS PAGE

18. Subject Terms (Continued)

Morphology, MoS₂
Lubrication model
X-ray diffraction of lubricant films
Intercrystalline slip, MoS₂

UNCLASSIFIED

SECURITY CLASSIFICATION OF THIS PAGE

PREFACE

This work was supported by the Defense Advanced Research Projects Agency and the United States Air Force, Contract Number F04701-85-C-0086. The authors are grateful to Dr. J. R. Lince and P. M. Adams for the XRD work and for helpful discussions, to J. L. Childs for the XPS measurements, and to S. L. McCluskey for the SEM photomicrographs. Thanks to Dr. W. E. Jamison, Durafilm Materials Corp., for assistance with some of the early concepts of the lubrication mechanism. The encouragement, criticism, and many insightful discussions with M. N. Gardos of the Hughes Aircraft Co. are also gratefully acknowledged.

Accession For	
NTIS GRA&I	<input checked="" type="checkbox"/>
DTIC TAB	<input type="checkbox"/>
Unannounced	<input type="checkbox"/>
Justification	
By	
Distribution/	
Availability Codes	
Dist	Avail and/or Special
A-1	



CONTENTS

PREFACE.....	1
I. INTRODUCTION.....	7
II. EXPERIMENTAL PROCEDURES.....	9
III. FILM CHARACTERIZATION.....	11
IV. SLIDING WEAR EXPERIMENTS.....	19
A. TRANSFER-FILM FORMATION.....	19
B. SURFACE CHEMISTRY OF WORN FILMS.....	22
C. STRUCTURAL VARIATION OF WORN FILMS.....	24
V. LUBRICATION MECHANISM.....	29
VI. CONCLUSIONS.....	33
REFERENCES.....	35

FIGURES

1.	X-ray photoelectron spectra of rf-sputtered MoS ₂ films, showing high-resolution Mo and S peaks after storage at high relative humidity and after wear of as-prepared (unstored) films.....	12
2.	The effect of varying stylus load on the measurement of film thickness.....	14
3.	SEM photomicrographs of HT films.....	15
4.	SEM photomicrographs of AT films.....	16
5.	SEM photomicrographs of transfer films on countersurfaces.....	20
6.	Variation in rf-sputtered MoS ₂ film composition as a function of sliding wear.....	23
7.	X-ray diffraction peaks for rf-sputtered MoS ₂ films as a function of the number of revolutions during sliding wear tests.....	25

TABLE

1.	Chemical and Structural Data for MoS ₂ Films as a Function of Sliding Wear.....	21
----	--	----

I. INTRODUCTION

Molybdenum disulfide, MoS_2 , is perhaps the best-known solid film lubricant for use in inert environments, including vacuum and space applications. Sputter deposition is a convenient method for achieving good adhesion to most substrates and good lubrication for relatively thin films ($\approx 1 \mu\text{m}$ thick). The resulting films perform excellently under relatively low contact stresses ($\sim 7\text{--}70,000 \text{ kPa}$) for rolling or sliding applications. However, loss of film material during wear and the lack of a suitable lubricant replenishment mechanism pose problems. Consequently, films must be produced with maximum wear lifetimes, minimum friction, and maximum resistance to environmental attack.

After more than 25 years of work on MoS_2 and other layered materials, relatively little fundamental information is available on the structural and chemical properties of such materials and on ways in which those properties influence lubrication properties and performance.¹ Early theories on lubrication mechanisms were derived primarily from friction and wear measurements and extrapolation from static properties.^{1,2} Structural studies showing crystal-lite orientation by means of x-ray diffraction for burnished films,³ and structural, morphological, and hardness studies of sputtered films have been reported.⁴⁻¹⁰ Surface chemical data for rubbed and sputtered films also have been reported.¹¹⁻¹⁸ There has even been an attempt to use electronic structure, as derived from molecular orbital (MO) theory, to interpret and predict lubricant performance.¹⁹

In a previous paper, we correlated results of surface chemical analyses with those of unidirectional, low load, sliding wear tests in an inert atmosphere and with transfer film formation. The resulting model attributed friction behavior to bulk film properties and film adhesion to interfacial chemical interactions.¹⁷ Sputtered MoS_2 films with partially oxidized surfaces (30 to 40% surface MoO_3) that contained small quantities of an oxidized sulfur species were demonstrated to have longer wear lives than those that were either not oxidized or that were oxidized more severely. Measurements

were made with films prepared on heated substrates (~ 230°C) and on cooler ones (~ 70°C). As part of that study, film morphology, grain size, and crystallite structure were speculated to influence wear behavior, possibly to a greater extent than surface chemical variations.

The present study is a continuation of that work. Results of surface chemical and structural measurements, made at various stages during the actual wear process, are combined with analyses of film morphology, density, and hardness to comprehensively assess sliding friction and wear behavior. A lubrication mechanism is proposed for optimal performance, involving sliding of MoS₂ crystallites over each other rather than cleavage of individual crystallites (i.e., inter- rather than intracrystallite slip). That randomly oriented films, type I,¹⁵ probably never become completely oriented during the sliding wear process is also shown. Crystal structure and electron density arguments are used to interpret observed variations in different films and to predict conditions for the preparation of films with desired properties and performance. [In this report, the term "crystallite" refers to individual single crystals, one or many of which constitute the platelet-shaped particles of the films. Whether individual crystallites or whole particles slide over each other is discussed. The crystallites can also be referred to as "sub-grains."]

II. EXPERIMENTAL PROCEDURES

Films of MoS_2 were prepared by rf sputter deposition according to procedures described previously.¹⁴⁻¹⁷ Substrates for the film samples, and countersurfaces for the wear tests, consisted of 440C steel flats polished to a mirror finish with alumina, final grit size 300 nm. The substrates were placed 36 mm from a 152 mm (6 in.) diameter, water-cooled MoS_2 target. The target was hot-pressed from 99.0% MoS_2 ; no structural analysis of the target was performed, but spectrographic analysis indicated the theoretical amount of Mo (59 wt%) and only small quantities of Si (0.15 wt%) and Fe (0.25 wt%) impurities. (Such analyses do not provide the sulfur concentrations.) Auger electron spectra of the deposited films evidenced neither Si nor Fe, indicating that their surface concentrations were $\sim 1\%$ of a monomolecular layer (monolayer).

The sputter target was mounted in the center of a 460 mm (18 in.) bell-jar vacuum system that was pumped with a liquid-nitrogen-trapped, oil diffusion pump [base pressure of 1.3×10^{-4} Pa (1×10^{-6} torr)]. Sputtering was performed with the rf planar diode power supply set at 350 W, equivalent to $1.93 \text{ W}\cdot\text{cm}^{-2}$, and an argon pressure of 2.4 to 2.7 Pa in the chamber. A residual gas analyzer was used for chamber gas analysis prior to admitting Ar and after pumping out the chamber after sputtering. Water was the major contaminant in both instances, with smaller amounts of N_2 , O_2 , Ar, CO_2 , SO_2 , and H_2S also present. SO_2 and H_2S tended to be at higher concentrations after sputtering than before.

The target was conditioned (presputtered onto a shutter) for approximately 100 min under the same sputtering parameters as for the actual depositions. A thermocouple, mounted adjacent to one of the substrates, monitored temperature, and a cartridge heater was installed into the substrate table to heat the substrates to a maximum of 340°C . Glass cover slides covered portions of some substrates to enable thickness measurements with a stylus profilometer (see Section III for a discussion of thickness measurements).

Film composition was observed to vary with the substrate temperature and with the usage of the sputtering system. Films deposited onto heated substrates ($> 200^{\circ}\text{C}$) were always of high purity, that is, greater than 90% MoS_2 . If the chamber, including the target, was unused but maintained at roughing pump vacuum (~ 13 Pa) for more than a month between sputter depositions, the ambient-temperature (AT) films (i.e., those deposited with no substrate temperature control, resulting in a substrate temperature of $\sim 70^{\circ}\text{C}$) contained approximately 30 mole% MoO_3 throughout, even with target conditioning. After three or four sputtering runs, the purity of such films increases and remains good as long as the system is operating or is kept under high vacuum; compositions comparable to the films prepared at high temperature, $>90\%$ MoS_2 , are achieved. In all cases, the major film impurity is MoO_3 . Only results for experiments with the high-purity films ($>90\%$ MoS_2) are reported here, but some films were stored in chambers maintained at elevated relative humidity (RH) and ambient temperature for various times before use.¹⁷ For films stored at high RH (85%) for relatively short times (up to six months), a very thin layer (~ 5 nm) of MoO_3 forms on the surface.

Films were characterized by scanning electron microscopy (SEM)²⁰ and x-ray photoelectron spectroscopy (XPS),¹⁷ and wear measurements¹⁷ were obtained by standard techniques with instrumentation described in the cited references. In addition, structural information for the films was obtained by means of x-ray diffraction (XRD) measurements (θ - 2θ scans) of as-prepared films and of those worn for various times.²⁰ For XPS measurements after periods of wear, the samples were maintained under dry nitrogen at all times until the sample analysis chamber was evacuated for the measurements. The stylus measurements were made with conventional instrumentation.

III. FILM CHARACTERIZATION

Three sets of films were prepared for this study: (1) Films sputtered onto substrates with no temperature control in the cleaned vacuum chamber and used immediately or after storage in a desiccator; they had mole fractions, F , of > 0.9 MoS_2 and are designated AT/F 0.9. (2) Films that were sputtered onto substrates with no temperature control in the clean system but were stored in an 85% RH atmosphere, resulting in surface layers with mole fractions (MoS_2) of ~ 0.75 (designated AT/SF 0.75). (3) Films sputtered onto substrates maintained at high temperature, between 230 and 320°C, all of which have F values greater than 0.9 (designated HT). The stated compositions were determined from XPS spectra, such as those in Fig. 1, by comparing the relative intensities of the Mo $3d_{5/2}$ peaks for the sulfide and oxide.^{15,17} The F values represent surface compositions, but comparison of the photoelectron spectroscopy data^{16,21} with the results of XRD, discussed in Section IV.B, indicates that the compositions for the films that were not intentionally oxidized by storage at high RH are typical of the entire film bulk as well as the surface. By contrast, those films that were stored at 85% RH had a thin layer of MoO_3 on their surfaces.

Major differences in morphological, structural, and chemical properties have been observed among films of the HT and AT categories.^{17,20} Initial scanning electron micrographs revealed that the particles in the HT films are substantially larger than those of the AT films.^{17,20} The surfaces (outer 5 nm) of the HT films were not oxidized during storage in ambient, humid atmospheres, whereas those of the AT films were 50% oxidized after 6 months' storage at 85% relative humidity.¹⁷ (See also Fig. 1.) Such findings indicate not only that the particles are larger for the HT films but that the crystallites within the particles are larger, too. If the particles simply had more crystallites of the same size as those of the AT films, the static oxidation would be comparable because it occurs along grain boundaries and on edge planes of the crystallites, and the relative edge-surface area-to-volume ratios would be the same for both AT and HT films.

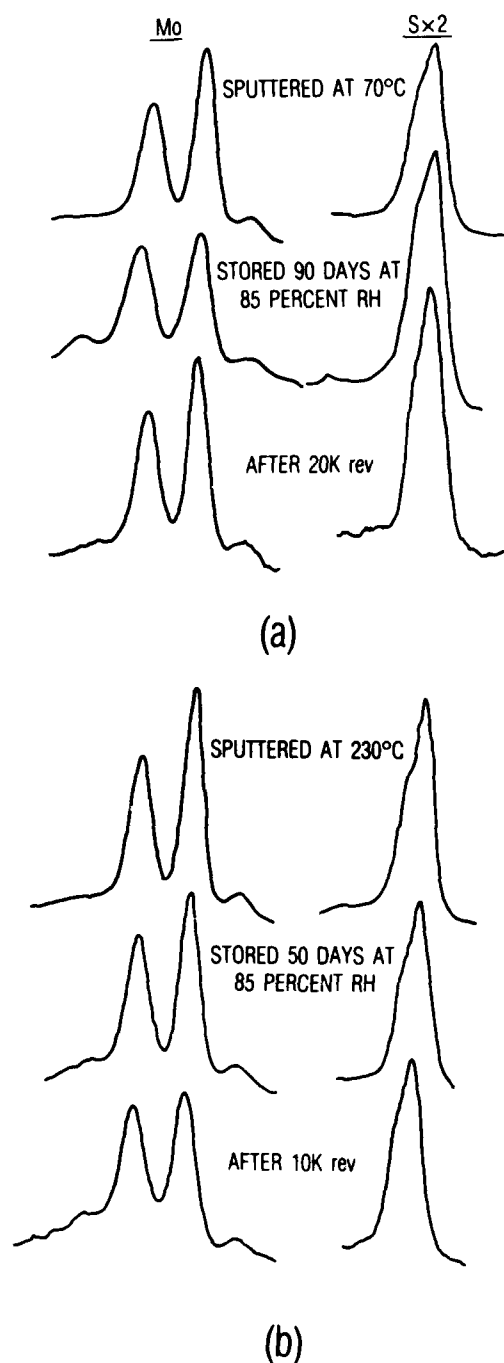


Fig. 1. X-ray photoelectron spectra of rf-sputtered MoS_2 films, showing high-resolution Mo and S peaks after storage at high relative humidity and after wear of as-prepared (unstored) films: (a) AT ($\sim 70^\circ\text{C}$) films and (b) HT ($\sim 230^\circ\text{C}$) films.

Thickness and density measurements were made by passing a stylus across steps in the films (Fig. 2) and by weighing. Those data, together with SEM observations of the stylus tracks (Figs. 3 and 4), provide additional information about the physical properties of the HT and AT film categories. Gardos has cautioned against the use of stylus techniques for measuring thicknesses of sputter-deposited MoS_2 films, showing that the depth of penetration of the stylus into the film at the step varies with the density of the film.⁴ Our results confirm that his concerns are valid, but they also indicate that varying the load on the stylus enables reasonably accurate thickness results and structural data for the films to be obtained.

A significant difference between HT and AT films is obvious from Figs. 2 through 4. The HT films are relatively soft and easily deformed by a single pass of the stylus, whereas the AT films are more dense and do not exhibit substantial deformation even at the higher stylus loads. For HT films, as the load on the stylus is increased, the apparent film thickness decreases and the degree of deformation within the stylus tracks increases markedly. From measurement of the track width in Fig. 3(e) for the 10 mg load condition and use of the ball diameter of the stylus tip, the penetration depth was calculated to be 100 nm, or about 20% of the estimated thickness of 500 nm. The most accurate thickness measurements using the stylus technique would be obtained by extrapolating measurements at different loads to the 0 mg value, but for convenience in this work the 10 mg value was used, making the determinations accurate to within approximately 20%.

Figure 3(a) depicts the surface of an HT film containing surface blemishes--regions where portions of the film are missing--immediately after preparation. (Our experience in preparing and analyzing many films is that sometimes such surface blemishes occur for no obvious reason, but that most films are continuous and uniform and look identical to the areas between the blemishes.) Clearly, the large particles of the HT films constitute one layer upon another layer of much smaller particles. The smaller particles appear to be almost the same size and shape as those found in the AT films, Fig. 4(a). Photomicrographs 3(b) and 3(c) show that the large particles are platelet shaped; the normal surface view of as-prepared films shows the edges of the

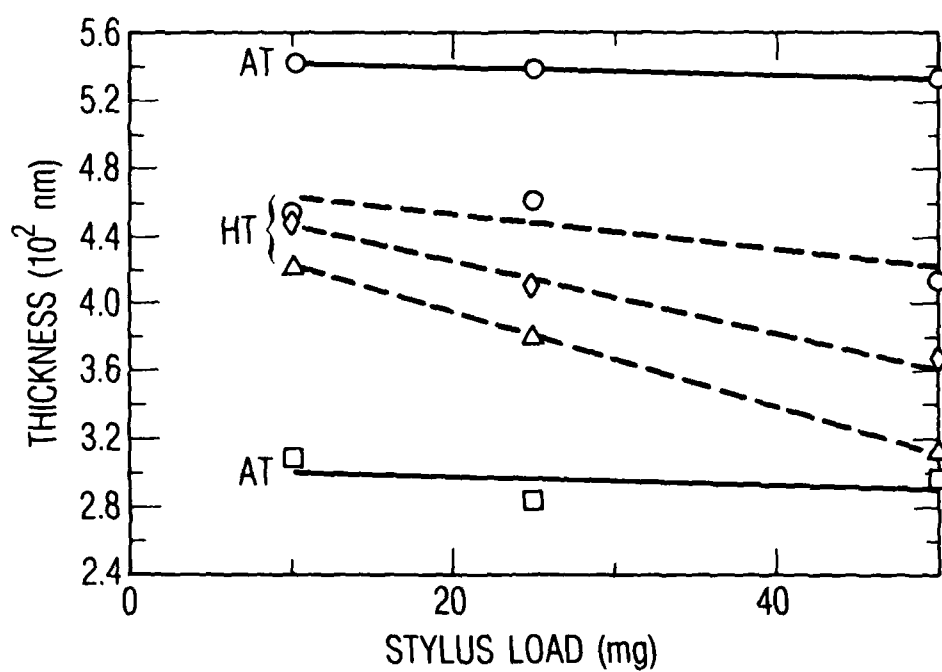


Fig. 2. The effect of varying stylus load on the measurement of film thickness.

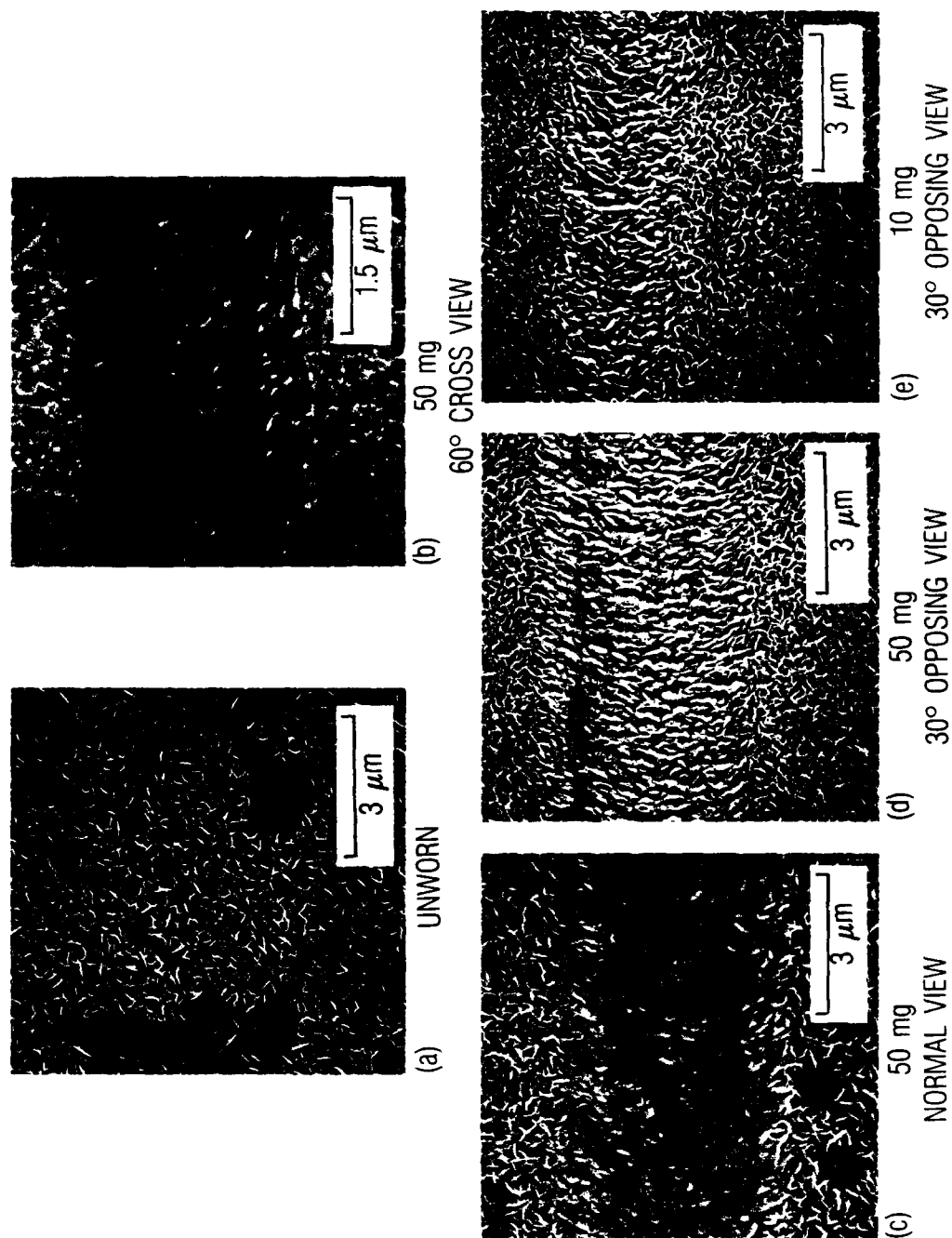


Fig. 3. SEM photomicrographs of HT films: (a) Unworn film, normal viewing; (b) 50 mg load stylus track viewed at a 60° angle across the track; (c) 50 mg track, normal view; (d) 50 mg track viewed at 30° angle opposing direction of sliding; and (e) 10 mg track, same view as (d).

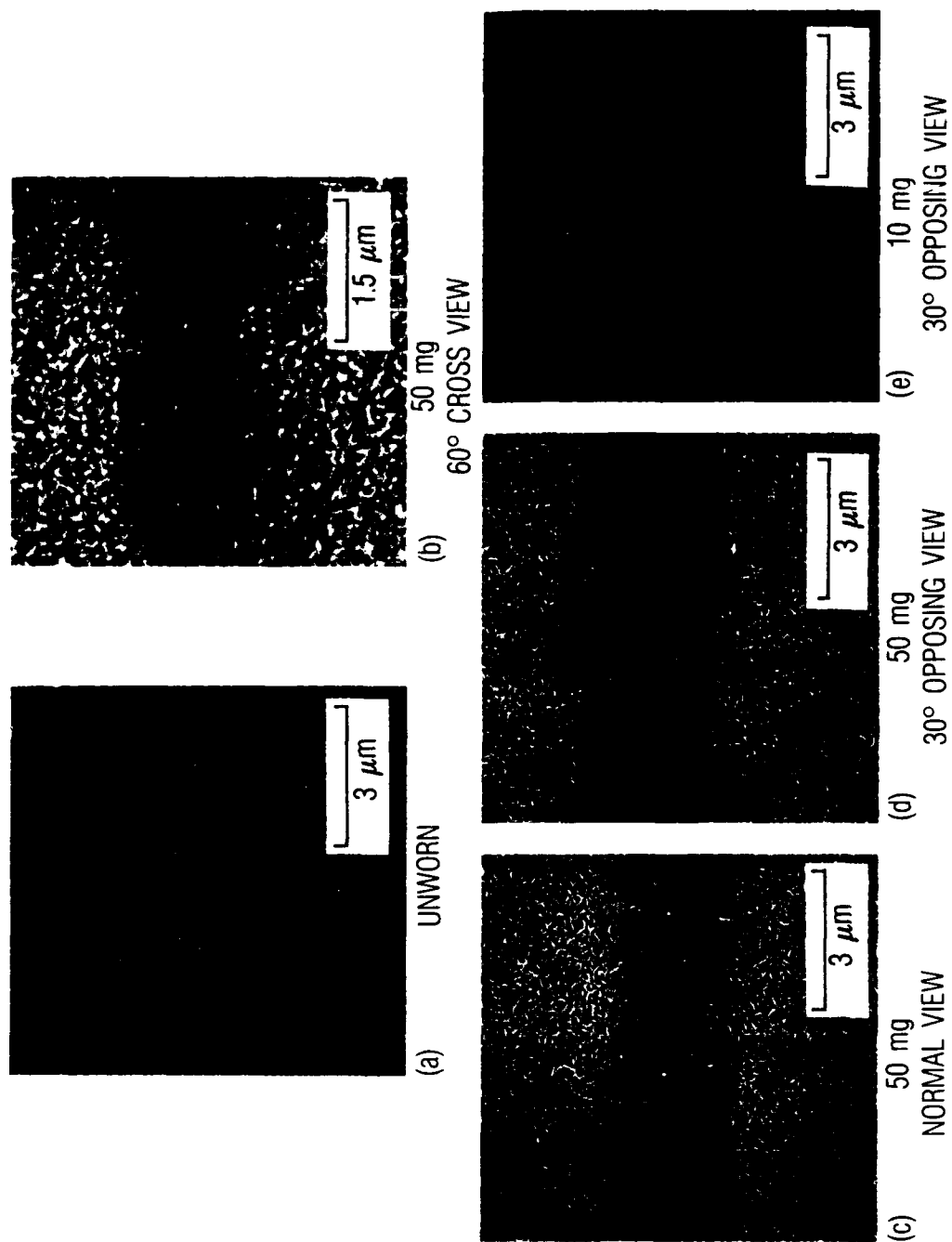


Fig. 4. SEM photomicrographs of AT films: (a) through (e) same as Fig. 3.

plates. Only after rubbing are the flat sides of the plates evident. Photomicrographs 3(d) and 3(e) were taken with the sample slightly tilted; the left side of the picture corresponds to the raised side of the sample, so that the view is into the trough opposed to the direction of sliding. (This technique emphasizes viewing of the plate edges.) The depth of penetration of the stylus for the 50 mg load was approximately 300 nm or ~ 60% into the film, whereas the depth for 10 mg was ~100 nm. The large plates in the HT films are easily burnished over to lie on their basal surfaces, and some plates may be fractured by the rubbing action.

The same conditions of stylus sliding on the AT films produced much less damage and little reorientation of the smaller platelets, Fig. 4. There are fewer differences between the 10 mg and 50 mg loads; the penetration depths correspond to 20 nm and 80 nm, respectively. The 50 mg track is approximately the same width and depth as that for 10 mg on the HT films, but the burnishing appears to be at the very surface only. The edge surfaces of particles beneath the track are still visible. The lack of variation in apparent thickness of the AT films with stylus load (Fig. 2) is consistent with the photomicrographs and indicates that the AT films are more dense, thereby appearing harder than the HT films. The measured densities are AT $3.0 \text{ mg}\cdot\text{mm}^{-3}$ and HT $1.9 \text{ mg}\cdot\text{mm}^{-3}$, compared with $4.9 \text{ mg}\cdot\text{mm}^{-3}$ for molybdenite. [Note that our films are significantly less dense than those of Buck,⁸ who reported $3.3 \text{ mg}\cdot\text{mm}^{-3}$ for amorphous, $3.8 \text{ mg}\cdot\text{mm}^{-3}$ for type I, and $3.95 \text{ mg}\cdot\text{mm}^{-3}$ for type II films.]

The structural characteristics of the HT films resemble those described by Spalvins:^{5,6} a layer of low-density, large particles ("columnar fiber zone") that appears to cover a layer of more dense, smaller particles ("equiaxed zone"). The AT films, on the other hand, appear to consist entirely of the more dense region. A major difference between our films and Spalvins' is that, upon sliding contact of reasonable load ($\sim 4.2 \times 10^4 \text{ kPa}$; 6 ksi), the large particles are burnished over and may be fractured, but they are not sloughed off the track as were those of Spalvins. The XRD results described in the next section provide more insight into the effects of sliding wear.

IV. SLIDING WEAR EXPERIMENTS

A. TRANSFER-FILM FORMATION

The sliding wear measurements were conducted with the same apparatus and under the same conditions as described previously.¹⁷ Briefly, the apparatus consisted of a disk sliding against a coated flat under low loads (3.18 kg dead-weight load) with a mean sliding velocity of $33 \text{ mm}\cdot\text{s}^{-1}$. The apparent contact area between the rider and the stationary member was approximately 45.2 mm^2 . In some tests, films were run until failure (arbitrarily defined as that point when the reaction torque of the stationary member exceeds $0.07 \text{ N}\cdot\text{m}$); other tests were terminated after a fixed number of revolutions, and chemical or structural measurements or both were made.

Data on the extent of coverage of the initially bare counterface as a function of the number of revolutions of the rotating, film-coated surface are listed in Table 1. The coverage factors were estimated from scanning electron micrographs like those in Fig. 5. Typically, a number of photomicrographs were taken of the subject surface. The areas of the portions covered with MoS_2 were measured and averaged to provide the percentages in Table 1. (A minimum of four different films were run for each set of conditions for various times and were then analyzed; specific films were not run, analyzed, and then rerun sequentially.) Significant differences are evident between HT and AT films and between surface preoxidized (SF 0.75) and unoxidized films. After only 1 rev, the HT films have covered almost 20% of the counterface, whereas the AT films cover less than 10%. However, as contact continues, coverage by the HT films increases very slowly, following essentially the same pattern as the unoxidized, AT/F 0.9, films until 10,000 rev, at which point the HT film coverage again increases. The initial, relatively high surface coverage for HT films is consistent with the burnishing of large platelets, observed with the SEM and discussed above, and with the XRD results discussed in Subsection IV.C.

As to the preoxidized/unoxidized film differences, the oxidized, AT/SF 0.75, films have a lower net coverage after 1 rev but increase their

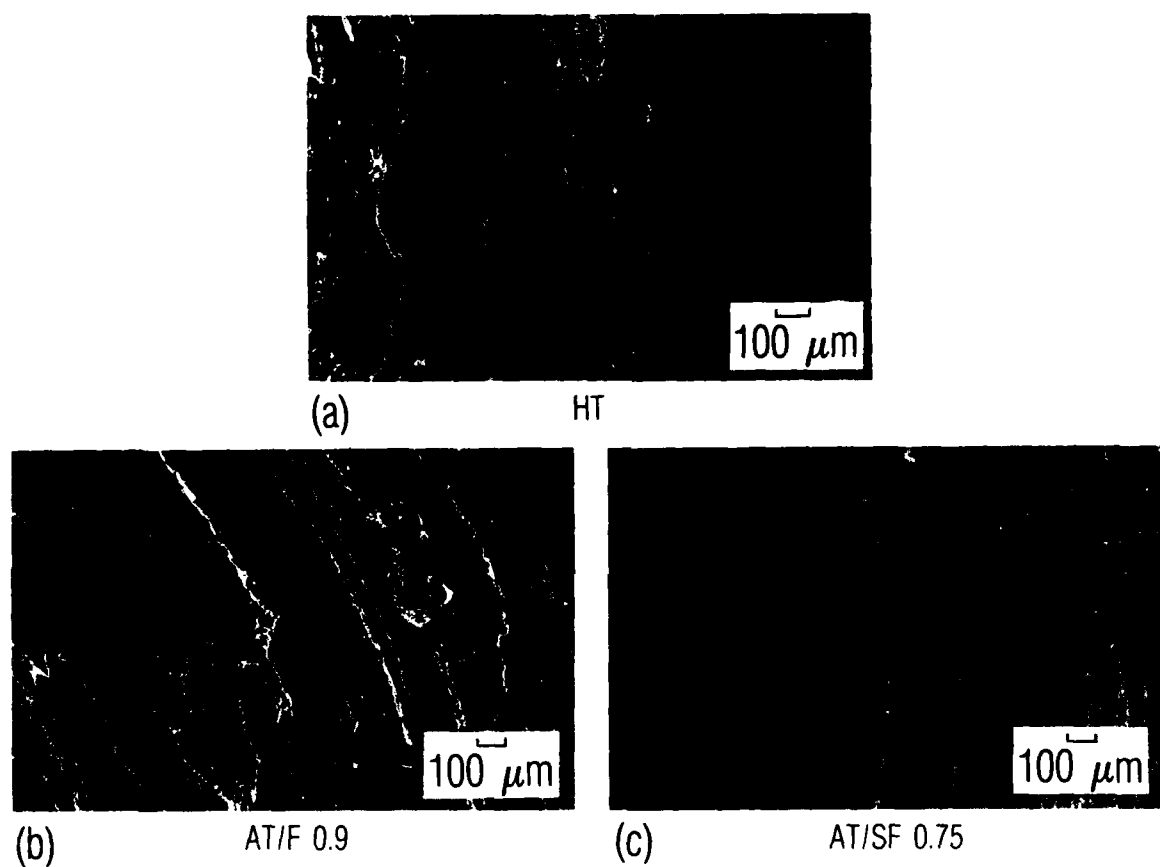


Fig. 5. SEM photomicrographs of transfer films on countersurfaces: (a) HT film after 1000 rev; (b) AT/F 0.9 film after 2000 rev; and (c) AT/SF 0.75 film after 1000 rev.

Table 1. Chemical and Structural Data for MoS₂ Films
as a Function of Sliding Wear

Number of Revolutions	Percent of Coverage ^a	F(MoS ₂) ^b	Percent of Edge Peak Maximum ^c	Percent of Basal Peak Maximum ^c
AT/F 0.9				
0	0	.90 - .94	100	0
1	1-7	.81 - .85	96	0
100	1-17	.85 - .89	76	15
2000	32-54	.89 - .93	40	69
20,000	40-60	.90 - .94	51	100
100,000	79-100	.82 - .86	40	58
AT/SF 0.75				
0	0	.71 - .79	100	0
1	1-17	.57 - .65	100	0
100	16-44	.64 - .72	100	8
1000	68-88	.65 - .73	86	17
10,000	91-100	.68 - .76	66	100
HT/F 0.9				
0	0	.92 - .98	100	0
1	5-25	.75 - .81	53	52
10	5-19	.80 - .86	38	100
100	18-30	.78 - .84	45	76
1000	18-44	.71 - .77	31	85
10,000	67-95	.63 - .69	35	100

^aAverage of ≥ 6 samples with error equal to ± 1 standard deviation from SEM.

^bAverage of 3 samples with error equal to range of values for unworn films from XPS.

^cCalculated from XRD peak heights.

coverage at a much higher rate than either the AT unoxidized or HT films. The SEM photomicrographs show that the transfer films for the AT/SF 0.75 films are uniform and evenly distributed over the countersurface, whereas those for the F 0.9 films are patchy and very thick in some areas but thin or nonexistent in other areas. The surface oxidized films attain 30% coverage after only 100 rev, 70% after 1000 rev, and >95% after 10,000 rev. The F 0.9 films (AT and HT) attain between 80 and 90% coverage at 100,000 rev, and transfer-film formation may not be complete even at failure, typically between 200,000 and 800,000 rev.

B. SURFACE CHEMISTRY OF WORN FILMS

The composition variable, $F(\text{MoS}_2)$, for the deposited MoS_2 films (not the transfer films) is plotted in Fig. 6 as a function of the number of sliding wear revolutions. Data for the figure were obtained from spectra such as those in Fig. 1. The films are composed of MoS_2 and MoO_3 , which means that $F(\text{MoO}_3)$ is equal to $1 - F(\text{MoS}_2)$ and the variation in $F(\text{MoO}_3)$ will be the inverse of that in Fig. 6. Again, major differences between HT and AT films are evident. For all films, the $F(\text{MoS}_2)$ decreases after only 1 rev. The fraction of MoS_2 for HT films increases slightly after 10 rev but then continues to decrease with further wear. Conversely, for the AT films, $F(\text{MoS}_2)$ increases after the initial drop to return approximately to its initial value and not decrease until near failure.

The initial contact with the bare, though oxidized counterface causes all of the MoS_2 films to oxidize rapidly under rubbing, even at low loads and in an inert environment. The presence of a preexisting surface oxide layer on the AT films does not appear to significantly alter initial oxidation, but it does result in the formation of a much more uniform transfer film on the counterface (see Subsection IV.A). The HT film was more or less continuously oxidized during wear but was not oxidized during storage in humid atmospheres.¹⁷

These seemingly contradictory phenomena are explained by the HT films' large particles (consisting of large crystallites) with very small edge-surface area-to-volume ratios, which do not react under the static conditions

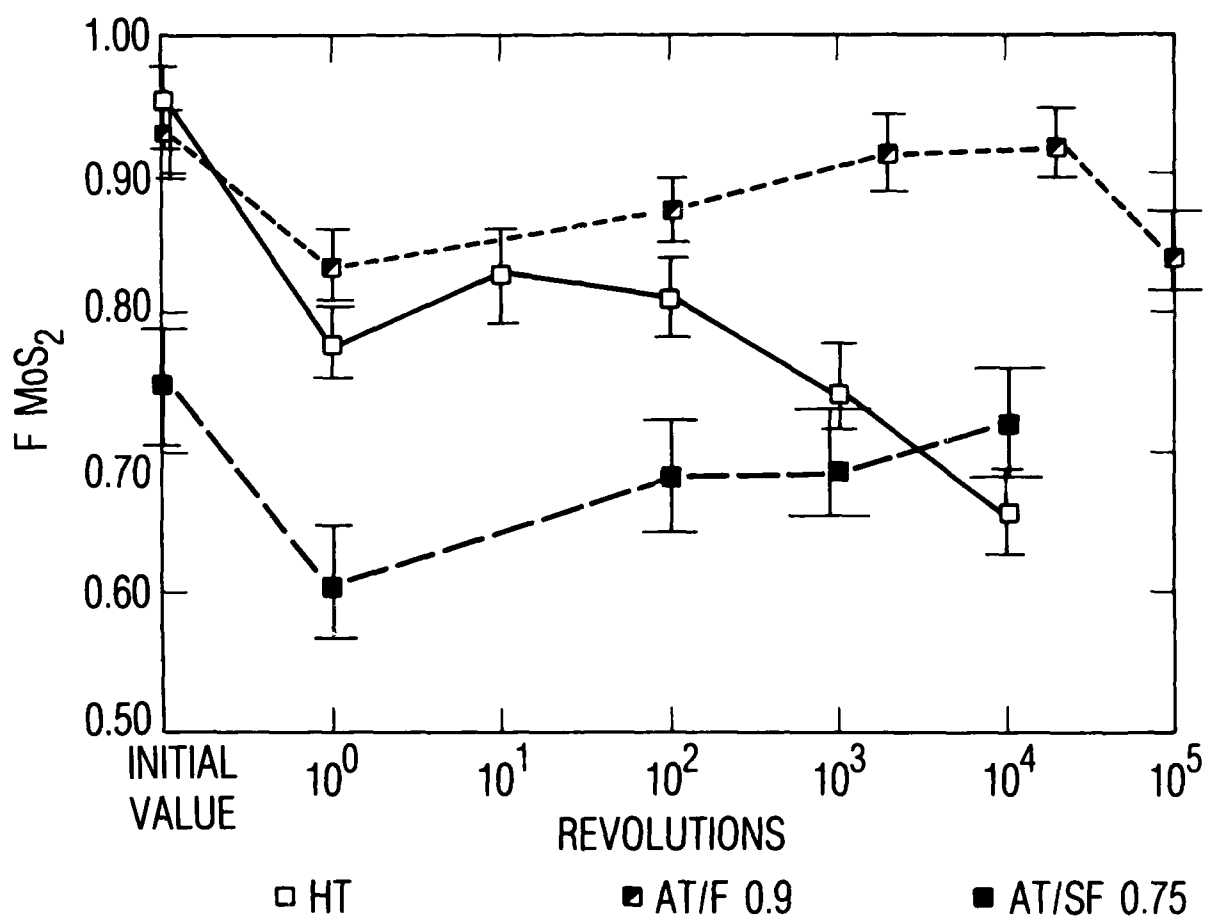


Fig. 6. Variation in rf-sputtered MoS_2 film composition as a function of sliding wear. Each data set (i.e., that for HT, AT/F 0.9, and AT/SF 0.9) represents films from a single sputter run. A single film was used for each point, with the exception of the initial values, which were determined for all of the films. The error bars on the points represent the ranges of the analyses for the unworn films.

of storage but which are fractured, continuously, during rubbing to create fresh, very reactive edge surfaces that are oxidized by the uncoated portions of the counterface (or possibly by traces of oxygen in the nitrogen purge gas). Conversely, the small particles of the AT films have substantial percentages of edge surface that react in storage, but the films are more compact (harder); the particles slide over each other and do not fracture and therefore do not produce new reactive surfaces during rubbing. The SEM photomicrographs of the stylus tracks (e.g., Fig. 4) show what appear to be layers of oriented particles (crystallites) that form during sliding of the AT films to cover the remainder of nonoriented particles within the films. The top layers in the wear experiments are thin (see the following subsection), but they probably protect the lower layers from oxidation even though the counterface may not be fully coated. .

C. STRUCTURAL VARIATIONS OF WORN FILMS

For proper lubricating action to be achieved, MoS_2 crystallites within a lubricating film must be oriented with their basal planes parallel to the plane of the contacting surfaces. Sputtered films can be prepared with that orientation.^{8,9,15} However, the conditions that produce proper orientation during preparation are not fully understood,^{8,9} and most sputtered films appear to contain crystallites oriented with their basal planes perpendicular to substrate surface planes. Sputtered films generally achieve correct orientation during burnishing or running-in, but such after-the-fact orientation probably does not result in the best lubrication or greatest durability.¹⁵ X-ray diffraction data (Fig. 7) for as-prepared films and films worn for various times again reveal significant differences between HT and AT films and provide insight into the film lubrication mechanism.

The x-ray diffractograms in Fig. 7 indicate that rubbing decreases the intensities of both (100) and (110) edge plane reflections, coincident with an increase in the (002) basal plane reflection. All reflections occur at angles slightly different from those for the molybdenite crystal, indicating corresponding differences in the d-spacings of the crystallites in various lattice directions. The "edge" [i.e., (hk0)] reflections occur at larger angles,

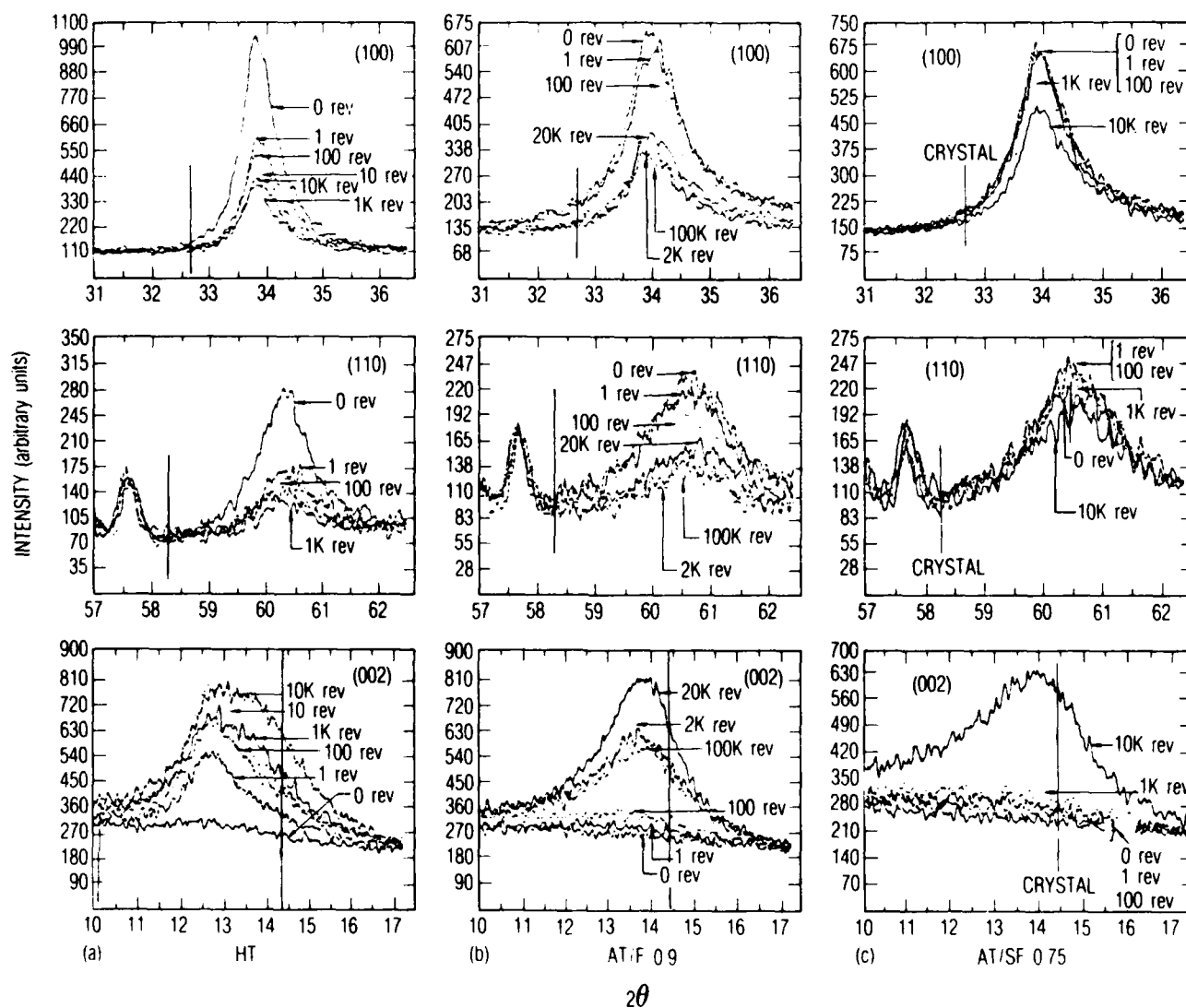


Fig. 7. X-ray diffraction peaks for rf-sputtered MoS_2 films as a function of the number of revolutions during sliding wear tests: (a) HT films; (b) AT/F 0.9 films; and (c) AT/SF 0.75 films.

indicating compression (smaller lattice spacings) in the directions perpendicular to edge planes, whereas the basal reflections are at smaller angles, showing expansion (larger spacing) in the $\langle 001 \rangle$ direction.

One revolution of the test fixture reduces the intensity of edge reflections of the HT films by almost 50%, and a clear basal plane reflection forms to almost 50% of its maximum intensity. (One revolution for the AT films produces barely detectable changes in any of the crystallographic directions.) Continued rubbing reduces the HT edge plane reflections and increases the basal reflections further; the changes in the edge direction reach an apparent steady state at ~ 35% of their initial value after only 10 to 100 rev, whereas changes in the basal direction appear to continue until failure.

A transformation occurs during the wear of the HT films and after the bulk of the film particles have been reoriented, that is, when wear-induced changes in the $\langle hk0 \rangle$ directions have reached the steady-state regime. The transformation involves crystallites of two distinctly different lattice spacings in the $\langle 001 \rangle$ direction (i.e., perpendicular to the basal plane). The initial stages of rubbing (up through 100 rev) produce oriented crystallites with relatively larger (001) spacing (2θ peak at 12.6°). Between 100 and 1000 rev, crystallites with spacings comparable to those produced by rubbing AT/F 0.9 (2θ peak at 13.7°) films begin to appear, until by 10,000 rev such crystallites dominate the diffractogram. Our speculation is that this change in lattice spacing corresponds to the fracturing of the larger initial crystallites within the HT films, that the oxidation shown in Fig. 6 occurs on the freshly formed edge surfaces [note the correspondence between increased oxidation and the appearance of the second (002) reflection at 100 rev], and that most wear of HT films involves slip of the fractured crystallites.

Changes in the reflections from the various planes of the AT films are, in contrast, gradual and depend largely on the pretreatment of the films (whether or not they have been exposed to humid storage environments to oxidize their outer surfaces). All AT films manifest a single basal reflection after rubbing, although the peak is broad, indicating strain within the crystallites or substantial variation in the lattice spacing for different

crystallites around the average value. The intensities of the edge plane reflections decrease more slowly than those of the HT films and again appear to reach a steady state; the steady-state point corresponds to an intensity of ~ 60% of the initial intensity for the surface-oxidized films and ~ 45% for the unoxidized films.

The increases in the basal plane reflections of the AT films are also slow and track the decreases in the edge directions. Differences between surface oxidized and unoxidized films are obvious for the basal reflections. The first 1000 rev produce barely detectable orientation for the oxidized films compared with a substantial (002) peak for the unoxidized films, a difference that is probably due to the formation of the relatively smooth, continuous transfer film on the counterface for the surface-oxidized film. The transfer film forms because of the better bonding and adhesion of the oxidized MoS_2 layers and provides a low-friction interface consisting of two films sliding on each other rather than one film rubbing against a substantially bare surface. The transfer process occurs before very much of the film in the contact zone has become oriented. Similar experiments need to be conducted at higher contact stresses (loads) to determine whether a larger fraction of the film becomes oriented.

Wear of the unoxidized AT film shows an initial increase in the intensity of the basal plane reflection that reaches a maximum value after approximately 20,000 rev. The decrease with further rubbing probably results from removal of material without orientation of the underlying crystallites. For all film types unoriented material is still present until failure, as shown by the data of Fig. 7 for the edge plane reflections. [The intensities of the (100) and (110) reflections for 100% oriented films would become ~ 20% of the initial value because the XRD analysis area is larger than the wear track area.] The persistence of unoriented crystallites during wear confirms our previous contention¹⁵ that the best lubricant films must be made directly in the oriented configuration without having to be burnished to achieve correct orientation.

V. LUBRICATION MECHANISM

All film morphology and hardness results and chemical and structural changes during wear are consistent with the proposition that the HT films contain one or more layers of large ($300 \pm 100 \text{ nm} \times 400 \pm 100 \text{ nm}$) particles over smaller ones (~ 100 to 150 nm on a side) and that the large particles burnish easily but are also fractured during rubbing to produce smaller particles that are readily oxidized.

The crystallites within the particles are distorted relative to natural molybdenite but appear to be of the same 2H poly type. The crystallites within the larger particles of the HT films have a larger (001) spacing (which is measurable after rubbing) than those of the AT films; the AT films are made up completely of the smaller particles. The larger d-spacing of the HT films provides for lower friction²² during the initial stages of rubbing. But, the transverse fracture (i.e., in a direction perpendicular to the large platelet surface) of the large HT particles appears to cause the crystallites to revert to the same (001) spacing as that of the small crystallites of the AT films. At the same time, because of the exposure of fresh edge surfaces, the smaller particles are oxidized (by the counterface or by trace contaminants), resulting in a thicker layer of oxide on the HT films during rubbing. The XRD results show that there is a thicker layer of burnished material during wear of the HT films: $\sim 65\%$ compared with 40% or 55% for the AT films.

The compositions of the AT films remain essentially unchanged (i.e., there is little oxidation); the crystallites are burnished very slowly, and no lattice spacing changes occur during rubbing. Conversely, films with initially large particles (HT films) burnish quickly, exhibit lattice relaxation toward the d-spacing of natural molybdenite, and are oxidized under the same rubbing conditions. Therefore, for the AT films under such stress conditions, the crystallites will not fracture transversely and lubrication will be achieved by the sliding of whole crystallites over each other, i.e., inter-crystallite slip. This slip mechanism appears to be the desired one, given the substantially longer wear lifetimes of AT films: 800,000 to 1,200,000 rev

for 500-nm-thick films compared with about 250,000 rev for 500-nm-thick HT films.

It is often argued that results such as these are valid only for the conditions of the specific test or application (i.e., contact stress, sliding or rolling speed). We propose that the only variable of consequence for MoS₂-type lubricant films is crystallite size, and that the process of producing optimal lubricant films begins with identifying the crystallite size that promotes the intercrystallite slip mechanism. Even if films are made so that they are preoriented,^{8,15} there is likely to be a proper crystallite size for a given set of operational conditions that produces intercrystallite slip and, therefore, maximum wear lifetime.

Demonstration of the intercrystallite slip mechanism of lubrication by sputtered MoS₂ films enables film performance to be expressed in terms of a fundamental material property of the system (i.e., crystallite size) and not in terms of sputtering or other preparation recipes, which can differ considerably from system to system.²³ Given the proper analytical tools and with this lubrication mechanism, one can determine the preparation conditions that provide the required values of the critical material property.

Even if this mechanism applies, some variations in film performance can still occur, necessitating proper orientation of as-prepared films. In addition to minimizing problems with oxidation, orientation will lengthen wear life by enabling graceful (i.e., noncatastrophic) wear of the entire film. The current films appear to fail when there is penetration through the film to a layer of rigidly bonded crystallites that cannot be burnished (oriented properly). Oxidation of the bulk of the film is a problem in any case and must be minimized. A useful modification to properly oriented films with appropriate crystallite size may be to artificially expand the lattice spacing in the $\langle 001 \rangle$ direction. Such expansion should reduce friction without reducing wear lifetime, and may be possible by doping the MoS₂ structure with metal ions such as those reported in Ref. 24. A qualitative molecular orbital description of the electronic structure of MoS₂²⁵ predicts that interlayer spacing in the $\langle 001 \rangle$ direction can be increased by reducing the electron

density in the d_{z^2} orbital of the Mo atom. To verify the predictions of our model, future work in our laboratory will be directed toward determining the influence of various metal dopants on the MoS_2 crystal and electronic structure.

VI. CONCLUSIONS

The longest wearing sputtered MoS_2 films lubricate by means of an inter-crystallite slip mechanism, whereby intact crystallites within the film slide over each other. Such sliding crystallites are not cleaved (fractured) in directions transverse to their basal planes because no new reactive surfaces are produced during wear. Films with larger particles and crystallites are cleaved until they attain the optimal particle and crystallite dimensions for a given set of operating conditions. A correlation between crystallite/particle size and use specifications must be established for maximum wear resistance. Subsequently, film deposition conditions for present and future applications must be selected on the basis of the achievement of the desired, optimal sizes. To realize new applications of MoS_2 dry film lubricants, future research must address friction-optimizing and oxidation-resistant properties within the context of maintaining particle size.

Even when films have the proper crystallite size, if they are prepared with the crystallites in the random orientation (type I), they probably never achieve complete basal plane orientation during sliding wear. This conclusion makes it imperative that methods for forming adhesive bonds to the basal surface be developed and fully understood before the best films can be produced.

REFERENCES

1. Winer, W. O., "Molybdenum Disulfide as a Lubricant: A Review of the Fundamental Knowledge," Wear, 10, pp 422-452 (1967); Lansdown, A. R., "Molybdenum Disulphide Lubrication. A Continuation Survey 1979-80," ESA TRIB/4 (ESTEC), 1983.
2. Holinski, R., and Gansheimer, J., "A Study of the Lubricating Mechanism of Molybdenum Disulfide," Wear, 19, pp 329-342 (1972).
3. Johnston, R. R. M., and Moore, A. J. W., "The Burnishing of Molybdenum Disulphide onto Metal Surfaces," Wear, 7, pp 498-512 (1964).
4. Gardos, M. N., "Quality Control of Sputtered MoS₂ Films," Lubr. Eng., 32, pp 463-580 (1976).
5. Spalvins, T., "Morphological and Frictional Behavior of Sputtered MoS₂ Films," Thin Solid Films, 96, pp 17-24 (1982).
6. Spalvins, T., "Frictional and Morphological Properties of Au-MoS₂ Films Sputtered from a Compact Target," Thin Solid Films, 118, pp 375-384 (1984).
7. Buck, V., "Morphological Properties of Sputtered MoS₂ Films," Wear, 91, pp 281-288 (1983).
8. Buck, V., "Structure and Density of Sputtered MoS₂-films," Vacuum, 36, pp 89-94 (1986).
9. Buck, V., "A Neglected Parameter (Water Contamination) in Sputtering of MoS₂ Films," Thin Solid Films, 139, pp 157-168 (1986).
10. Bichsel, R., and Levy, F., "Morphological and Compositional Properties of MoSe₂ Films Prepared by R.F. Magnetron Sputtering," Thin Solid Films, 16, pp 367-372 (1984).
11. Atkinson, I. B., and Swift, P., "A Study of the Tribochemical Oxidation of Molybdenum Disulphide Using X-ray Photoelectron Spectroscopy," Wear, 29, pp 129-133 (1974).
12. Buckley, D. H., "Examination of Molybdenum Disulfide with LEED and Auger Emission Spectroscopy," NASA TN D-7010, December 1970.
13. Bichsel, R., Levy, F., and Mathieu, H. J., "Study of R. F. Magnetron-sputtered MoSe₂ Films by Electron Spectroscopy for Chemical Analysis," Thin Solid Films, 131, pp 87-94 (1985).

14. Stewart, T. B., and Fleischauer, P. D., "Chemistry of Sputtered Molybdenum Disulfide Films," Inorg. Chem., 21, pp 2426-2431 (1982).
15. Fleischauer, P. D., "Effects of Crystallite Orientation on the Environmental Stability and Lubrication Properties of Sputtered MoS₂ Thin Films," ASLE Trans., 27, pp 82-88 (1984).
16. Fleischauer, P. D., and Tolentino, L. U., "Structural Studies of Sputtered MoS₂ Films by Angle Resolved Photoelectron Spectroscopy," Proc. 3rd ASLE Int. Solid Lubr. Conf., 1984, Denver, CO, ASLE SP-14, pp 223-229.
17. Fleischauer, P. D., and Bauer, R., "The Influence of Surface Chemistry on MoS₂ Transfer Film Formation," ASLE Trans., 30, pp 160-166 (1987).
18. Dimigen, H., Hübsch, H., Willich, P., and Reichelt, K., "Stoichiometry and Friction Properties of Sputtered MoS_x Layers," Thin Solid Films, 129, pp 79-91 (1985).
19. Z. Gu, "A Discussion of the Relationship Between the Structure of the Transition Metal Dichalcogenides and their Lubrication Performance," ASLE Trans., 25, pp 207-212 (1982).
20. Lince, J. R., and Fleischauer, P. D., Crystallinity of RF-Sputtered MoS₂ Films, TR-0086A(2945-03)-2, The Aerospace Corporation, El Segundo, California (15 April 1988).
21. Fleischauer, P. D., and Stewart, T. B., Effects of Crystallite Orientation on the Oxidation of MoS₂ Thin Films, TR-0084A(5945-03)-2, The Aerospace Corporation, El Segundo, California (9 September 1985).
22. Jamison, W. E., "Structure and Bonding Effects on the Lubricating Properties of Crystalline Solids," ASLE Trans., 15, pp 296-305 (1972); Jamison, W. E., "Intercalated Dichalcogenide Solid Lubricants," ASLE SP-14, pp 73-87 (1984).
23. Gardos, M. N., and Meeks, C. R., Solid Lubricated Rolling Element Bearings, AFWAL-TR-83-4129, Part I, Vol. 1, p 51, and Part II, Vol. 1, pp 78, 216 (February 1984).
24. Stupp, B. C., "Synergistic Effects of Metals Co-Sputtered with MoS₂," Thin Solid Films, 84, pp 257-266 (1981).
25. Haycock, D. E., Urch, D. S., and Wiech, G., "Electronic Structure of Molybdenum Disulphide," J. Chem. Soc., Faraday Trans. 2, 75, pp 1692-1702 (1979). See also Fleischauer, P. D., Proc. 14th Int. Conf. Metallurgical Coatings, 23-27 March 1987, San Diego, California (1987).

LABORATORY OPERATIONS

The Aerospace Corporation functions as an "architect-engineer" for national security projects, specializing in advanced military space systems. Providing research support, the corporation's Laboratory Operations conducts experimental and theoretical investigations that focus on the application of scientific and technical advances to such systems. Vital to the success of these investigations is the technical staff's wide-ranging expertise and its ability to stay current with new developments. This expertise is enhanced by a research program aimed at dealing with the many problems associated with rapidly evolving space systems. Contributing their capabilities to the research effort are these individual laboratories:

Aerophysics Laboratory: Launch vehicle and reentry fluid mechanics, heat transfer and flight dynamics; chemical and electric propulsion, propellant chemistry, chemical dynamics, environmental chemistry, trace detection; spacecraft structural mechanics, contamination, thermal and structural control; high temperature thermomechanics, gas kinetics and radiation; cw and pulsed chemical and excimer laser development including chemical kinetics, spectroscopy, optical resonators, beam control, atmospheric propagation, laser effects and countermeasures.

Chemistry and Physics Laboratory: Atmospheric chemical reactions, atmospheric optics, light scattering, state-specific chemical reactions and radiative signatures of missile plumes, sensor out-of-field-of-view rejection, applied laser spectroscopy, laser chemistry, laser optoelectronics, solar cell physics, battery electrochemistry, space vacuum and radiation effects on materials, lubrication and surface phenomena, thermionic emission, photo-sensitive materials and detectors, atomic frequency standards, and environmental chemistry.

Computer Science Laboratory: Program verification, program translation, performance-sensitive system design, distributed architectures for spaceborne computers, fault-tolerant computer systems, artificial intelligence, microelectronics applications, communication protocols, and computer security.

Electronics Research Laboratory: Microelectronics, solid-state device physics, compound semiconductors, radiation hardening; electro-optics, quantum electronics, solid-state lasers, optical propagation and communications; microwave semiconductor devices, microwave/millimeter wave measurements, diagnostics and radiometry, microwave/millimeter wave thermionic devices; atomic time and frequency standards; antennas, rf systems, electromagnetic propagation phenomena, space communication systems.

Materials Sciences Laboratory: Development of new materials: metals, alloys, ceramics, polymers and their composites, and new forms of carbon; non-destructive evaluation, component failure analysis and reliability; fracture mechanics and stress corrosion; analysis and evaluation of materials at cryogenic and elevated temperatures as well as in space and enemy-induced environments.

Space Sciences Laboratory: Magnetospheric, auroral and cosmic ray physics, wave-particle interactions, magnetospheric plasma waves; atmospheric and ionospheric physics, density and composition of the upper atmosphere, remote sensing using atmospheric radiation; solar physics, infrared astronomy, infrared signature analysis; effects of solar activity, magnetic storms and nuclear explosions on the earth's atmosphere, ionosphere and magnetosphere; effects of electromagnetic and particulate radiations on space systems; space instrumentation.